Crucial lncRNAs associated with adipocyte differentiation from human adipose-derived stem cells based on co-expression and ceRNA network analyses

Kana Chen [1], **Shujie Xie** [2], **Wujun Jin** [Corresp. 1]

[1] Department of Plastic Surgery, Hwa Mei Hospital, University of Chinese Academy of Sciences, Ningbo, Zhejiang, China

[2] Department of Hepatobiliary Surgery, Hwa Mei Hospital, University of Chinese Academy of Sciences, Ningbo, Zhejiang, China

Corresponding Author: Wujun Jin
Email address: wujunjin2019@163.com

Background: Injection of adipose derived stem cells (ASCs) is a promising treatment for facial contour deformities. However, its treatment mechanisms remain largely unknown. The study aimed to explain the molecular mechanisms of adipogenic differentiation from ASCs based on the roles of long noncoding RNAs (lncRNAs).

Methods: Datasets of mRNA-lncRNA (GSE113253) and miRNA (GSE72429) expression profiling were collected from Gene Expression Omnibus database. The differentially expressed genes (DEGs), lncRNAs (DELs) and miRNAs (DEMs) between undifferentiated and adipocyte differentiated human ASCs were identified using the LIMMA method. DELs related co-expression and competing endogenous RNA (ceRNA) networks were constructed. Protein-protein interaction (PPI) analysis was performed to screen crucial target genes.

Results: A total of 748 DEGs, 17 DELs and 51 DEMs were identified. Thirteen DELs and 279 DEGs with Pearson correlation coefficients > 0.9 and p-value < 0.01 were selected to construct the co-expression network. A total of 151 interaction pairs among 112 nodes (10 DEMs; 8 DELs; 94 DEGs) were obtained to construct the ceRNA network. By comparing the lncRNAs and mRNAs in two networks, five lncRNAs (SNHG9, LINC02202, UBAC2-AS1, PTCSC3 and MIAT) and 32 genes (i.e. such as PIK3R1, PTPRB) were found to be shared. PPI analysis demonstrated PIK3R1 , FOXO1 (a transcription factor), and ESR1 were hub genes, which could be regulated by the miRNAs that interacted with the above five lncRNAs, such as LINC02202-miR-136-5p-PIK3R1, LINC02202-miR-381-3p-FOXO1 and MIAT-miR-18a-5p-ESR1. LINC02202 also could directly co-express with PIK3R1. Furthermore, PTPRB was predicted to be modulated by co-expression with LINC01119.

Conclusion: MIAT, LINC02202 and LINC01119 may be potentially important, new lncRNAs associated with adipogenic differentiation of ASCs. They may be involved in adipogenesis by acting as a ceRNA or co-expressing with their targets.

Crucial lncRNAs associated with adipocyte differentiation from human adipose-derived stem cells based on co-expression and ceRNA network analyses

Kana Chen[1], Shujie Xie[2], Wujun Jin[1]*

[1]Department of Plastic Surgery, Hwa Mei Hospital, University of Chinese Academy of Sciences, Ningbo, Zhejiang, 315010, China;

[2]Department of Hepatobiliary Surgery, Hwa Mei Hospital, University of Chinese Academy of Sciences, Ningbo, Zhejiang, 315010, China.

*Corresponding author: Wujun Jin.

Email: wujunjin2019@163.com; Telephone: +86-13780088664.

Corresponding address: Department of Plastic Surgery, Hwa Mei Hospital, University of Chinese Academy of Sciences, Haishu District, No.41 Northwest Street, Ningbo, Zhejiang, 315010, China.

Abstract

Background: Injection of adipose derived stem cells (ASCs) is a promising treatment for facial contour deformities. However, its treatment mechanisms remain largely unknown. The study aimed to explain the molecular mechanisms of adipogenic differentiation from ASCs based on the roles of long noncoding RNAs (lncRNAs).

Methods: Datasets of mRNA-lncRNA (GSE113253) and miRNA (GSE72429) expression profiling were collected from Gene Expression Omnibus database. The differentially expressed genes (DEGs), lncRNAs (DELs) and miRNAs (DEMs) between undifferentiated and adipocyte differentiated human ASCs were identified using the LIMMA method. DELs related co-expression and competing endogenous RNA (ceRNA) networks were constructed. Protein-protein interaction (PPI) analysis was performed to screen crucial target genes.

Results: A total of 748 DEGs, 17 DELs and 51 DEMs were identified. Thirteen DELs and 279 DEGs with Pearson correlation coefficients > 0.9 and p-value < 0.01 were selected to construct the co-expression network. A total of 151 interaction pairs among 112 nodes (10 DEMs; 8 DELs; 94 DEGs) were obtained to construct the ceRNA network. By comparing the lncRNAs and mRNAs in two networks, five lncRNAs (SNHG9, LINC02202, UBAC2-AS1, PTCSC3 and MIAT) and 32 genes (i.e. such as PIK3R1, PTPRB) were found to be shared. PPI analysis demonstrated PIK3R1, FOXO1 (a transcription factor), and ESR1 were hub genes, which could be regulated by the miRNAs that interacted with the above five lncRNAs, such as LINC02202-miR-136-5p-PIK3R1, LINC02202-miR-381-3p-FOXO1 and MIAT-miR-18a-5p-ESR1. LINC02202 also could directly co-express with PIK3R1. Furthermore, PTPRB was predicted to be modulated by co-expression with LINC01119.

Conclusion: MIAT, LINC02202 and LINC01119 may be potentially important, new lncRNAs associated with adipogenic differentiation of ASCs. They may be involved in adipogenesis by

acting as a ceRNA or co-expressing with their targets.

Key words: Human adipose tissue-derived stromal stem cells; adipogenic differentiation; ceRNA; lncRNA; miRNA; co-expression

Introduction

Autologous adipose tissue grafting has been a widely accepted surgical tool for anti-aging cosmetics (Charles-de-Sá L 2015) and reconstructive restoration of various congenital or acquired facial soft tissue deformities (Bashir et al. 2018). However, conventional fat grafting procedure needs to be repeated multiple times to achieve satisfactory results (Bashir et al. 2018), which may be associated with the low graft survival rate and poor revascularization (Ma L 2015). To overcome these two limitations, recent scholars propose to combine with additional autologous adipose-derived stem cells (ASCs) which have the ability to differentiate into mature adipocytes to supplement apoptotic cells and secrete angiogenic growth factors to enhance angiogenesis (Bashir et al. 2018; Kotaro et al. 2008; Philips et al. 2014). The clinical trials also confirm that supplementation of ASCs to adipose grafts is superior to conventional lipoinjection for facial recontouring (Bashir et al. 2018; Kotaro et al. 2008). Nevertheless, the use of autologous ASCs has not been FDA-approved. This may be because there still remains a huge gap in understanding the potential mechanisms of ASCs for adipocyte differentiation.

Increasing evidence has suggested long noncoding RNAs (lncRNAs), a class of noncoding RNAs more than 200 nucleotides, play crucial roles in adipogenesis for ASCs. For example, Nuermaimaiti et al. demonstrated that knockdown of HOXA11-AS1 inhibited adipocyte differentiation, leading to suppression of adipogenic-related gene transcription, as well as decreased lipid accumulation in ASCs (Nuermaimaiti et al. 2018). Huang et al. observed knockdown of MIR31HG inhibited adipocyte differentiation, whereas overexpression of MIR31HG promoted adipogenesis *in vitro* and *in vivo* (Huang et al. 2017). MEG3 was also found to be downregulated during adipogenesis of ASCs. Functional analysis showed that knockdown of MEG3 promoted adipogenic differentiation of ASCs (Zheng et al. 2017). Furthermore, current research shows lncRNAs, on one hand, functions as microRNA (miRNAs)

sponges to bind the miRNA response elements (MREs) and regulate miRNA-mediated gene silencing [that is, competing endogenous RNA (ceRNA) hypothesis]; and, on the other hand, directly influences their neighboring genes expression by chromatin remodeling or transcriptional control (co-expression model)(Huang et al. 2016; Li et al. 2017). These theories have also been reported in ASCs. Li et al. proved downregulated MEG3 may be insufficient to sponge miR-140-5p and lead to its upregulation during adipogenesis in ASCs (Zheng et al. 2017). The study of Huang et al. revealed inhibition of MIR31HG reduced the enrichment of active histone markers, histone H3 lysine 4 trimethylation and acetylation, in the promoter of fatty acid binding protein 4, resulting in suppression of its expression and adipogenesis (Huang et al. 2017). However, the adipogenic differentiation related lncRNAs and its mechanisms of ASCs remains rarely reported.

The present study aimed to identify crucial lncRNAs involved in adipocyte differentiation of ASCs by constructing lncRNA-miRNA-mRNA ceRNA network and lncRNA-mRNA co-expression network using high throughput analysis data. Our findings might offer greater insights into the molecular mechanisms of adipocyte differentiation from ASCs and provide potentially new targets for inducing adipogenesis.

Materials and methods

Collection of microarray data

GSE113253 (Rauch et al. 2019) and GSE72429 datasets (Supplemental Information 1) were downloaded from the Gene Expression Omnibus (GEO) database (http://www.ncbi.nlm.nih.gov/geo/). GSE113253 dataset applied the high throughput sequencing methodology to simultaneously detect the lncRNA and mRNA expression profiles in 2 repeats of undifferentiated human ASCs and 10 repeats of adipogenic differentiation cells using an Illumina HiSeq 1500 instrument, which was submitted to GEO on Apr 17, 2018. GSE72429 dataset analyzed the miRNA expression profile in 4 undifferentiated human ASCs and 2 adipogenic differentiation cells using an Agilent-031181 Unrestricted_Human_miRNA_V16.0_Microarray (miRBase release 16.0 miRNA ID version), which was submitted to GEO on Aug 27, 2015.

Differential expression analysis

The normalized series matrix files of each dataset were downloaded from GEO. Following re-annotation according to corresponding platform (GPL18460), the expression values of the lncRNAs and mRNAs in GSE113253 were obtained. The differentially expressed genes (DEGs), lncRNAs (DELs) and miRNAs (DEMs) were identified using the Linear Models for Microarray Data (LIMMA) method software (version 3.34.0; https://bioconductor.org/packages/release/bioc/html/limma.html). P-value was adjusted by using Benjamini-Hochberg method to avoid false positives. The heatmap was constructed to present the expression difference of DEGs, DELs and DEMs in different samples using the pheatmap package (version: 1.0.8; https://cran.r-project.org/web/packages/pheatmap) based on Euclidean distance.

Co-expression network between lncRNA and mRNA

The co-expression network was constructed based on the correlation analysis between DELs and DEGs. Pearson correlation coefficients were calculated using the WGCNA (Weighted Gene Correlation Network Analysis; https://horvath.genetics.ucla.edu/html/CoexpressionNetwork/Rpackages/WGCNA/Tutorials/) algorithm to assess the correlation. Only the co-expressed pairs with absolute value of Pearson correlation coefficients ≥ 0.9 and $p < 0.01$ were selected to draw the network using Cytoscape (version 3.4; www.cytoscape.org/) (Kohl et al. 2011).

CeRNA regulatory network among DELs, DEMs and DEGs

The DEMs related target genes were predicted using the miRwalk database (version 2.0; http://www.zmf.umm.uni-heidelberg.de/apps/zmf/mirwalk2) (Dweep & Gretz 2015) which provides 12 prediction algorithms (miRWalk, MicroT4, miRanda, miRBridge, miRDB, miRMap, miRNAMap, PICTAR2, PITA, RNA22, RNAhybrid , Targetscan). Only the miRNA-target gene interaction pairs that were predicted in at least 8 databases were used. The target genes were then overlapped with the DEGs to screen negatively correlated DEM-DEG interaction pairs. The miRcode (http://www.mircode.org/)(Ashwini et al. 2012), starBase (version 2.0;

http://starbase.sysu.edu.cn/starbase2/) (Li et al. 2014) and DIANA-LncBase (version 2.0; http://carolina.imis.athena-innovation.gr/diana_tools/web/index.php?r=lncbasev2/index-predicted)(Paraskevopoulou et al. 2013) databases were used to predict the interaction relationship between DELs and DEMs. The negatively correlated DEL-DEM interaction pairs were left for further analysis. The DEL-DEM and DEM-DEG interactors were integrated to construct the ceRNA network, which was visualized using Cytoscape.

Protein-protein interaction (PPI) network

PPI data of DEGs in the ceRNA network was collected from STRING (Search Tool for the Retrieval of Interacting Genes; version 10.0; http://string db.org/) database (Szklarczyk et al. 2015). Only interactions with combined score > 0.4 were selected to construct the PPI network. Several topological features of the nodes (protein) in the PPI network were calculated using the CytoNCA plugin in cytoscape software (http://apps.cytoscape.org/apps/cytonca) (Tang et al. 2015) to screen hub genes, including degree, eigenvector, betweenness and closeness centrality. Furthermore, transcription factors were predicted using iRegulon (Janky et al. 2014) in Cytoscape and then integrated to the PPI network.

Function enrichment analysis

Gene ontology (GO) and Kyoto Encyclopedia of Genes and Genomes (KEGG) pathway enrichment analyses were performed using the Database for Annotation, Visualization and Integrated Discovery (DAVID) online tool (version 6.8; http://david.abcc.ncifcrf.gov) (Huang et al. 2009) to reveal the function of DEGs. $P < 0.05$ was set as the cut-off value.

Results

Differential expression analysis

Due to the fact that fewer DEGs, DELs and DEMs were identified if adjusted p-value was defined as the statistical threshold; therefore, genes, lncRNAs and miRNAs were believed to be differentially expressed in this study when their |log2fold change (FC)| was more than 1 and p-value was less than 0.05. Based on these given thresholds, a total of 748 protein-coding genes (360, upregulated; 388, downregulated)(Table 1;Supplemental Information 2) and 17 lncRNAs

(9, upregulated; 8, downregulated) (Table 1; Supplemental Information 2) were found to be differentially expressed in adipogenic differentiation cells compared with undifferentiated cells in GSE113253 dataset. Among them, 121 DEGs [such as FOXO1 (forkhead box O1), PTPRB (protein tyrosine phosphatase receptor type B)] and 2 DELs (SH3RF3-AS1, LINC01119) had adjusted p-value < 0.05, indicating they were especially crucial for adipogenic differentiation. A total of 51 miRNAs (Table 1; Supplemental Information 2) were identified to be significantly differentially expressed in GSE72429 within the $p < 0.05$ and $|log2FC| > 1$ criteria. Among them, 20 DEMs (particularly, miR-663 and miR-3607-3p, with adjusted p-value < 0.05) were upregulated and 31 DEMs (particularly, miR-150*, miR-4271, miR-371-5p and miR-134, with adjusted p-value < 0.05) were downregulated. Additionally, hierarchical clustering of DEGs (Figure 1A), DELs (Figure 1B) and DEMs (Figure 1C) expression levels indicated the differentiated samples could be well distinguished from the undifferentiated samples.

Construction of co-expression and ceRNA networks

A total of 13 DELs and 279 DEGs with Pearson correlation coefficients > 0.9 and p-value < 0.01 were selected to construct the lncRNA-mRNA co-expression network, which contained 440 positive connections (Figure 2; Supplemental Information 3).

Based on at least 8 database analyses in miRwalk 2.0 and negatively correlated principles, a total of 79 downregulated DEGs were predicted to be regulated by 8 upregulated DEMs, while 128 upregulated DEGs were predicted to be regulated by 32 downregulated DEMs. Using the starBase database, 355 miRNAs were predicted to interact with 25 DELs; using the miRcode database, 192 miRNAs were predicted to interact with 8 DELs; using the DIANA-LncBase database, 1343 miRNAs were predicted to interact with 15 DELs. After overlapping the DEMs that interacted with DELs and DEMs that regulated DEGs, 151 interaction pairs among 112 nodes (10 DEMs, 4 upregulated and 6 downregulated; 8 DELs, 4 upregulated and 4 downregulated; 94 DEGs, 46 upregulated and 48 downregulated) were obtained, which were used for constructing the ceRNA network (Figure 3; Supplemental Information 4).

PPI network

PPI pairs were predicted for the 94 DEGs in the ceRNA network using the STRING database, which resulted in 80 interaction relationship pairs that were screened between 58 nodes (24 upregulated and 34 downregulated) (Figure 4). PIK3R1 (phosphoinositide-3-kinase regulatory subunit 1), FYN (FYN proto-oncogene, Src family tyrosine kinase) and ESR1 (estrogen receptor 1) were considered as hub genes in the PPI network because they ranked the top 10 in all four topological features (Table 2). In addition, FOXO1, which was included in the PPI network, was predicted as a differentially expressed transcription factor to regulate the other target genes in the PPI network using IRegulon plug-in (Figure 4), indicating FOXO1 was also a hub gene.

Function analysis showed 8 significant KEGG pathways were enriched, including hsa04015:Rap1 signaling pathway (PIK3R1), hsa05200:Pathways in cancer (PIK3R1, FOXO1), hsa05205:Proteoglycans in cancer (ESR1, PIK3R1), hsa04014:Ras signaling pathway (PIK3R1), hsa05218:Melanoma (PIK3R1) and hsa04520:Adherens junction (PTPRB) (Table 3).

In addition, 79 GO biological process terms were also enriched, such as GO:0042981~regulation of apoptotic process (ESR1), GO:0045893~positive regulation of transcription, DNA-templated (ESR1, FOXO1), GO:0043066~negative regulation of apoptotic process (FOXO1, PIK3R1), GO:0014066~regulation of phosphatidylinositol 3-kinase signaling (PIK3R1), GO:0048146~positive regulation of fibroblast proliferation (ESR1), GO:0001525~angiogenesis (PTPRB) and GO:0001678~cellular glucose homeostasis (FOXO1, PIK3R1) (Table 4; Supplemental Information 5).

Integrated analysis to identify crucial lncRNAs

By comparing the co-expression with ceRNA networks, five lncRNAs (SNHG9, LINC02202, UBAC2-AS1, PTCSC3 and MIAT) and 32 genes (such as PIK3R1, PTPRB) were found to be shared.

By comparing the hub genes enriched into KEGG pathways with the genes regulated by the above five lncRNAs (SNHG9, LINC02202, UBAC2-AS1, PTCSC3 and MIAT), we found the following ceRNA and co-expression axes may be important, including LINC02202

(upregulated)-hsa-miR-136-5p (downregulated)-PIK3R1 (upregulated), LINC02202 (upregulated)-hsa-miR-381-3p (downregulated)-FOXO1 (upregulated), MIAT (downregulated)-hsa-miR-18a-5p (upregulated)-ESR1 (downregulated) and LINC02202 (downregulated)-PIK3R1(downregulated). Furthermore, the comparison between hub genes enriched into KEGG pathways and the shared genes in two networks also indicated PTPRB related co-expression axis [(LINC01119 (downregulated)-PTPRB (downregulated)] was also crucial.

Discussion

In present study, we identified three crucial lncRNAs (MIAT, LINC02202, and LINC01119) for adipogenesis from human ASCs. MIAT may sponge hsa-miR-18a-5p and influence the inhibition of hsa-miR-18a-5p on the expression of ESR1. LINC02202 may function as a ceRNA for hsa-miR-136-5p/hsa-miR-381-3p to respectively regulate the expressions of PIK3R1 and FOXO1; LINC02202 also may directly affect the transcription of PIK3R1. LINC01119 may co-express with PTPRB to impact its transcription. Although all these relationship pairs may be potentially important, LINC01119-PTPRB co-expression axis may be especially verifiable because their expression significance met the criterion of adjusted p-value < 0.05.

Although there have studies to show the roles of lncRNA myocardial infarction associated transcript (MIAT) for stem differentiation, only osteogenic (Jin et al. 2017) and endothelial cell (Wang et al. 2018) differentiation were investigated, without evidence to prove its effect on adipogenesis of human ASCs. A recent study revealed MIAT was an estrogen-inducible lncRNA and its expression was positively related to estrogen receptor (Li et al. 2018b). There was accumulating evidence to reveal that exposure of bone marrow stem cells to icariin or flavonoids of Herba Epimedii inhibited adipogenic differentiation, exhibiting decreased adipocyte numbers and downregulated mRNA expression of adipogenic differentiation markers, peroxisome proliferator-activated receptor gamma (PPARγ) and CCAAT/enhancer-binding protein α (C/EBPα)(Li X 2018; Zhang et al. 2015); while treatment of bone marrow stem cells with estrogen receptor antagonist ICI182780 revered the effects of Herba Epimedii ingredient and promoted adipogenesis (Li X 2018; Zhang et al. 2015). The study of Ihunnah et al. also

243 demonstrated activation of estrogen receptor in ASCs inhibited adipogenesis by decreasing the
244 recruitment of the adipogenic PPARγ onto its target gene promoters, whereas the use of estrogen
245 receptor antagonism ICI 182780 or knockdown of estrogen receptor-α via lentiviral shRNA
246 enhanced adipogenesis by increasing the expression of PPARγ (Ihunnah et al. 2014). Thus, it can
247 be hypothesized that MIAT may be lower expressed in adipogenic differentiation cells like ESR1,
248 which was also confirmed in our study. However, the interaction mechanisms between MIAT
249 and estrogen receptor remain unclear. In present study, we predicted that downregulated MIAT
250 may be insufficient to sponge hsa-miR-18a-5p and lead to more hsa-miR-18a-5p to bind with the
251 3′ untranslated region (3′UTR) of ESR1, inducing the lower expression of ESR1. This hypothesis
252 may be indirectly demonstrated by the fact that miR-18a mimic significantly promoted MSC
253 adipogenic differentiation, while the addition of miR-18a inhibitor obtained the negative effects
254 on adipogenic differentiation of mesenchymal stem cells (MSCs) (Li et al. 2018a). The negative
255 regulatory relationship between ESR1 and miR-18a were also validated in human trophoblast
256 cell line by the luciferase assay (Zhu et al. 2015).
257 LINC02202 may be a newly identified lncRNA associated with stem cell differentiation
258 because its role had not been previously mentioned in the literatures. In this study, we predicted
259 upregulated LINC02202 may be involved in ASCs adipogenic differentiation by regulating
260 phosphatidylinositol 3-kinase (PI3K) signaling. It has been reported that PI3K signaling pathway
261 was strongly activated in MSCs under the adipogenesis-inducing hormone cocktail (Kim et al.
262 2017), and the addition of PI3K specific inhibitor LY294002 severely suppressed lipid
263 accumulation, as well as the expression of adipogenic markers PPARγ and C/EBPα (Yu et al.
264 2008). PIK3R1 is a critical component of the PI3K signaling pathway and its expression was also
265 demonstrated to be increased after the induction of adipocyte differentiation from preadipocytes
266 3T3-L1 (Kim et al. 2014). Thus, theoretically, PIK3R1 may be upregulated in adipogenic
267 differentiation cells compared with undifferentiated human ASCs, which was confirmed in our
268 study. Activated PI3K/AKT signaling may promote adipogenesis through upregulating
269 downstream transcription factors, such as FoxO1 (Yi et al. 2018) which may subsequently

enhance the transcription of its target genes, PPAR-γ and C/EBP-α (Ambele et al. 2016; Munekata & Sakamoto 2009); whereas persistent inhibition of FoxO1 with its antagonist AS1842856 (Zou et al. 2014) or knockdown of FoxO1 (Sun et al. 2017) was also observed to almost completely suppress adipocyte differentiation and lipogenesis. As expected, we also found FoxO1 was significantly high expressed during adipogenic differentiation. In addition to directly affect the transcription of PIK3R1, LINC02202 may function as a ceRNA for miR-136-5p and hsa-miR-381-3p to regulate the expression of PIK3R1a and FoxO1, respectively. Although there was no study to demonstrate these ceRNA interaction axes, the negative correlation between the expression of miR-136 and adipogenic markers C/EBPα and PPARα in subcutaneous adipose tissue of lambs may indirectly illuminate the importance of miR-136 for adipogenic differentiation (Meale et al. 2014). As expected, we also found miR-136-5p was significantly downregulated in adipogenic differentiation cells.

There was only one sequencing study to identify that LINC01119 was downregulated in colorectal cancer cells after hypoxia treatment (Han et al. 2014). Several authors had demonstrated hypoxia exposure was effective to enhance adipocyte differentiation from ASCs (Fink et al. 2004; Valorani et al. 2012; Kim et al. 2013), which was medicated by the generation of reactive oxygen species (ROS) and activation of PI3K/Akt/mTOR (Kim et al. 2014); the addition of ROS scavenger or Akt/mTOR inhibitor prevented adipocyte differentiation (Kim et al. 2014). Thus, LINC01119 may have anti-adipose differentiation potential and lower expressed in adipogenic differentiation cells compared with undifferentiated human ASCs, which was validated in our study. However, its mechanisms for adipocyte differentiation remain unclear. We predicted LINC01119 may co-express with PTPRB. The study of Kim et al. showed ectopic over-expression of PTPRB inhibited the expression of adipocyte-related genes (such as PPAR-γ) and led to a reduced adipocyte differentiation from preadipocytes. Also, PTPRB was reported to suppress the tyrosine phosphorylation of VEGFR2 during adipocyte differentiation (Kim et al. 2019). Generally, VEGF functions by binding with VEGFR2, while transfection of VEGF to ASCs increased fat cell survival (Zhang et al. 2017). These findings suggest PTPRB may also be

297 downregulated to promote VEGF secretion and activate its mediated pathways, ultimately
298 inducing adipogenic differentiation from ASCs. This hypothesis was in line with our study
299 showing PTPRB was lower expressed in adipocyte differentiation cells and was involved in
300 angiogenesis.

301 There are some limitations in this study. First, only two datasets submitted within five years
302 until now, not all were used for this analysis, which may cause some bias in results due to the
303 small sample size and different data platforms. However, we believe the sequencing or
304 microarray technology may be more mature recently and thus the results may be more believable.
305 This was also indirectly reflected by the less overlapped genes if the other datasets were used
306 [only two comparing GSE72429 with GSE25715 (Guo et al. 2019)] and thus, we renounced the
307 use of multiple datasets and only the newly one. Moreover, this work investigated lncRNA co-
308 expression and ceRNA mechanisms, which required the lncRNA and mRNA should be
309 simultaneously analyzed. Thus, some datasets that only independently investigated lncRNA or
310 mRNA were also excluded. Second, the crucial co-expression and ceRNA axes were obtained by
311 database prediction, which may lead to many false positives. Therefore, further *in vitro* wet
312 experiments (PCR, luciferase assay, knockdown or overexpression) are still indispensable to
313 confirm the interaction between lncRNAs and miRNAs, lncRNA and mRNAs as well as the
314 miRNAs and mRNAs and their roles during adipogenic differentiation of ASCs.

315 **Conclusion**

316 The present study preliminarily identified three new targets (lncRNA MIAT, LINC02202
317 and LINC01119) for inducing of adipogenesis from human ASCs and promoting facial soft
318 tissue reconstruction. They may be involved in adipogenesis by acting as a ceRNA (LINC02202-
319 miR-136-5p-PIK3R1, LINC02202-miR-381-3p-FOXO1 and MIAT-miR-18a-5p-ESR1) or co-
320 expressing with its targets (LINC02202-PIK3R1, LINC01119-PTPRB).

321 **Availability of data and materials**

322 Raw data is available in Supplemental Materials (Supplemental Information 1).

323 **References**

Ambele MA, Dessels C, Durandt C, and Pepper MS. 2016. Genome-wide analysis of gene expression during adipogenesis in human adipose-derived stromal cells reveals novel patterns of gene expression during adipocyte differentiation. *Stem Cell Res* 16:725-734.

Ashwini J, Marks DS, and Erik L. 2012. miRcode: a map of putative microRNA target sites in the long non-coding transcriptome. *Bioinformatics* 28:2062-2063.

Bashir MM, Sohail M, Bashir A, Khan FA, Jan SN, Imran M, Ahmad FJ, and Choudhery MS. 2018. Outcome of Conventional Adipose Tissue Grafting for Contour Deformities of Face and Role of Ex Vivo Expanded Adipose Tissue-Derived Stem Cells in Treatment of Such Deformities. *J Craniofac Surg* 29:1143-1147.

Charles-de-Sá L, Gontijo-de-Amorim NF, Maeda Takiya C, Borojevic R, Benati D, Bernardi P, Sbarbati A, Rigotti G. 2015. Antiaging treatment of the facial skin by fat graft and adipose-derived stem cells. *Plast Reconstr Surg* 135:999-1009.

Dweep H, and Gretz N. 2015. miRWalk2. 0: a comprehensive atlas of microRNA-target interactions. *Nat Methods* 12:697.

Fink T, Abildtrup L, Fogd K, Abdallah BM, Kassem M, Ebbesen P, Zachar V. 2004. Induction of adipocyte-like phenotype in human mesenchymal stem cells by hypoxia. Stem Cells 22:1346-1355.

Guo Z, Cao Y. 2019. An lncRNA-miRNA-mRNA ceRNA network for adipocyte differentiation from human adipose-derived stem cells. Mol Med Rep 19:4271-4287.

Han Y, Wang X, Mao E, Shen B, Huang L. 2019. Analysis of Differentially Expressed lncRNAs and mRNAs for the Identification of Hypoxia-Regulated Angiogenic Genes in Colorectal Cancer by RNA-Seq. *Med Sci Monit* 18;25:2009-2015.

Huang DW, Sherman BT, and Lempicki RA. 2009. Systematic and integrative analysis of large gene lists using DAVID bioinformatics resources. *Nat Protoc* 4:44-57.

Huang M, Zhong Z, Lv M, Shu J, Tian Q, and Chen J. 2016. Comprehensive analysis of differentially expressed profiles of lncRNAs and circRNAs with associated co-expression and ceRNA networks in bladder carcinoma. *Oncotarget* 7:47186-47200.

351 Huang Y, Jin C, Zheng Y, Li X, Shan Z, Zhang Y, Jia L, and Li W. 2017. Knockdown of
352 lncRNA MIR31HG inhibits adipocyte differentiation of human adipose-derived stem
353 cells via histone modification of FABP4. *Sci Rep* 7:8080.
354 Ihunnah CA, Wada T, Philips BJ, Ravuri SK, Gibbs RB, Kirisci L, Rubin JP, Marra KG, Xie W.
355 2014. Estrogen sulfotransferase/SULT1E1 promotes human adipogenesis. *Mol Cell Biol*
356 34:1682-1694.
357 Janky R, Verfaillie A, Imrichová H, Van de Sande B, Standaert L, Christiaens V, Hulselmans G,
358 Herten K, Naval SM, and Potier D. 2014. iRegulon: from a gene list to a gene regulatory
359 network using large motif and track collections. *PLoS Comput Biol* 10:e1003731.
360 Jin C, Zheng Y, Huang Y, Liu Y, Jia L, and Zhou Y. 2017. Long non-coding RNA MIAT
361 knockdown promotes osteogenic differentiation of human adipose-derived stem cells.
362 *Cell Biol Int* 41:33-41.
363 Kim J, Han D, Byun SH, Kwon M, Cho SJ, Koh YH, Yoon K. Neprilysin facilitates
364 adipogenesis through potentiation of the phosphatidylinositol 3-kinase (PI3K) signaling
365 pathway. Mol Cell Biochem 2017, 430(1-2):1-9.
366 Kim JH, Kim SH, Song SY, Kim WS, Song SU, Yi T, Jeon MS, Chung HM, Xia Y, Sung JH.
367 2014. Hypoxia induces adipocyte differentiation of adipose-derived stem cells by
368 triggering reactive oxygen species generation. Cell Biol Int 38:32-40.
369 Kim JS, Kim WK, Oh KJ, Lee EW, Han BS, Lee SC, Bae KH. 2019. Protein Tyrosine
370 Phosphatase, Receptor Type B (PTPRB) Inhibits Brown Adipocyte Differentiation through
371 Regulation of VEGFR2 Phosphorylation. J Microbiol Biotechnol 29:645-650.
372 Kim YJ, Kim HJ, Chung KY, Choi I, Kim SH. 2014. Transcriptional activation of PIK3R1 by
373 PPARγ in adipocytes. *Mol Biol Rep* 41:5267-5272.
374 Kohl M, Wiese S, and Warscheid B. 2011. Cytoscape: software for visualization and analysis of
375 biological networks. *Methods Mol Biol* 696:291-303.
376 Kotaro Y, Katsujiro S, Noriyuki A, Masakazu K, Keita I, Hirotaka S, Hitomi E, Harunosuke K,
377 Toshitsugu H, and Kiyonori H. 2008. Cell-assisted lipotransfer for facial lipoatrophy:

efficacy of clinical use of adipose-derived stem cells. *Dermatol Surg* 34:1178-1185.

Li JH, Liu S, Zhou H, Qu LH, and Yang JH. 2014. starBase v2.0: decoding miRNA-ceRNA, miRNA-ncRNA and protein-RNA interaction networks from large-scale CLIP-Seq data. *Nucleic Acids Res* 42:D92-97.

Li M, Xie Z, Wang P, Li J, Liu W, Tang SA, Liu Z, Wu X, Wu Y, and Shen H. 2018a. The long noncoding RNA GAS5 negatively regulates the adipogenic differentiation of MSCs by modulating the miR-18a/CTGF axis as a ceRNA. *Cell Death Dis* 9:554.

Li X, Ao J, and Wu J. 2017. Systematic identification and comparison of expressed profiles of lncRNAs and circRNAs with associated co-expression and ceRNA networks in mouse germline stem cells. *Oncotarget* 8:26573-26590.

Li X, Peng B, Pan Y, Wang P, Sun K, Lei X, Ou L, Wu Z, Liu X, Wang H, He H, Mo S, Tian Y, Peng X, Zhu X, Zhang R, Yang L. 2018. Icariin stimulates osteogenic differentiation and suppresses adipogenic differentiation of rBMSCs via estrogen receptor signaling. *Mol Med Rep* 18:3483-3489.

Li Y, Jiang B, Wu X, Huang Q, Chen W, Zhu H, Qu X, Xie L, Ma X, and Huang G. 2018b. Long non-coding RNA MIAT is estrogen-responsive and promotes estrogen-induced proliferation in ER-positive breast cancer cells. *Biochem Biophys Res Commun* 503:45-50.

Ma L, Wen H, Jian X, Liao H, Sui Y, Liu Y, Xu G. 2015. Cell-assisted lipotransfer in the clinical treatment of facial soft tissue deformity. *Plast Surg* 23:199-202.

Meale SJ, Romao JM, He ML, Chaves AV, Mcallister TA, and Guan LL. 2014. Effect of diet on microRNA expression in ovine subcutaneous and visceral adipose tissues. *J Anim Sci* 92:3328-3337.

Munekata K, and Sakamoto K. 2009. Forkhead transcription factor Foxo1 is essential for adipocyte differentiation. *In Vitro Cell Dev Biol Anim* 45:642-651.

Nuermaimaiti N, Liu J, Liang X, Jiao Y, Zhang D, Liu L, Meng X, and Guan Y. 2018. Effect of lncRNA HOXA11-AS1 on adipocyte differentiation in human adipose-derived stem cells.

Biochem Biophys Res Commun 495:1878-1884.

Paraskevopoulou MD, Georgakilas G, Kostoulas N, Reczko M, Maragkakis M, Dalamagas TM, and Hatzigeorgiou AG. 2013. DIANA-LncBase: experimentally verified and computationally predicted microRNA targets on long non-coding RNAs. *Nucleic Acids Res* 41:D239-245.

Philips BJ, Marra KG, and Rubin JP. 2014. Healing of grafted adipose tissue: current clinical applications of adipose-derived stem cells for breast and face reconstruction. *Wound Repair Regen* 22:11-13.

Rauch A, Haakonsson AK, Madsen JGS, Larsen M, Forss I, Madsen MR, Van Hauwaert EL, Wiwie C, Jespersen NZ, Tencerova M, Nielsen R, Larsen BD, Röttger R, Baumbach J, Scheele C, Kassem M, Mandrup S. 2019. Osteogenesis depends on commissioning of a network of stem cell transcription factors that act as repressors of adipogenesis. *Nat Genet* 51:716-727.

Sun YM, Qin J, Liu SG, Cai R, Chen XC, Wang XM, and Pang WJ. 2017. PDGFRα Regulated by miR-34a and FoxO1 Promotes Adipogenesis in Porcine Intramuscular Preadipocytes through Erk Signaling Pathway. *Int J Mol Sci* 18:2424.

Szklarczyk D, Franceschini A, Wyder S, Forslund K, Heller D, Huerta-Cepas J, Simonovic M, Roth A, Santos A, and Tsafou KP. 2015. STRING v10: protein-protein interaction networks, integrated over the tree of life. *Nucleic Acids Res* 43:D447-452.

Tang Y, Li M, Wang J, Pan Y, and Wu FX. 2015. CytoNCA: a cytoscape plugin for centrality analysis and evaluation of protein interaction networks. *Biosystems* 127:67-72.

Valorani MG, Montelatici E, Germani A, Biddle A, D'Alessandro D, Strollo R, Patrizi MP, Lazzari L, Nye E, Otto WR, Pozzilli P, Alison MR. 2012. Pre-culturing human adipose tissue mesenchymal stem cells under hypoxia increases their adipogenic and osteogenic differentiation potentials. Cell Prolif 45:225-238.

Wang H, Ding XG, Yang JJ, Li SW, Zheng H, Gu CH, Jia ZK, and Li L. 2018. LncRNA MIAT facilitated BM-MSCs differentiation into endothelial cells and restored erectile

dysfunction via targeting miR-200a in a rat model of erectile dysfunction. *Eur J Cell Biol* 97:180-189.

Yi L, Chen J, Tao X, Zhou Y, Yuan W, Wang M, Gan Y, Wang K, Xiong S, and Cong M. 2018. Epigallocatechin-3-gallate suppresses differentiation of adipocytes via regulating the phosphorylation of FOXO1 mediated by PI3K-AKT signaling in 3T3-L1 cells. *Oncotarget* 9:7411-7423.

Yu W, Chen Z, Zhang J, Zhang L, Ke H, Huang L, Peng Y, Zhang X, Li S, and Lahn BT. 2008. Critical role of phosphoinositide 3-kinase cascade in adipogenesis of human mesenchymal stem cells. *Mol Cell Biochem* 310:11-18.

Zhang D, Liu L, Jia Z, Yao X, and Yang M. 2015. Flavonoids of Herba Epimedii stimulate osteogenic differentiation and suppress adipogenic differentiation of primary mesenchymal stem cells via estrogen receptor pathway. *Pharm Biol* 54:954-963.

Zhang Y, Xiao LL, Li JX, Liu HW, Li SH, Wu YY, Liao X, Rao CQ. 2017. Improved fat transplantation survival by using the conditioned medium of vascular endothelial growth factor transfected human adipose-derived stem cells. Kaohsiung J Med Sci 33:379-384.

Zheng L, Jin C, Si C, Zheng Y, Huang Y, Jia L, Ge W, and Zhou Y. 2017. Long non-coding RNA MEG3 inhibits adipogenesis and promotes osteogenesis of human adipose-derived mesenchymal stem cells via miR-140-5p. *Mol Cell Biochem* 433:51-60.

Zhu X, Yang Y, Han T, Yin G, Gao P, Ni Y, Su X, Liu Y, and Yao Y. 2015. Suppression of microRNA-18a expression inhibits invasion and promotes apoptosis of human trophoblast cells by targeting the estrogen receptor α gene. *Mol Med Rep* 12:2701-2706.

Zou P, Liu L, Zheng L, Liu L, Stoneman RE, Cho A, Emery A, Gilbert ER, Cheng Z. 2014. Targeting FoxO1 with AS1842856 suppresses adipogenesis. *Cell Cycle* 13:3759-3767.

459
460
461
462
463
464
465
466
467
468
469
470
471
472
473
474
475
476
477
478
479
480
481
482

Figure legends

Figure 1 Hierarchical clustering and heat map analysis of differentially expressed (A) genes, (B) long non-coding RNAs and microRNAs (C). The color to red, high expression; the color to light

blue, low expression.

Figure 2 Co-expression network between differentially expressed long non-coding RNAs and genes. A, downregulated lncRNA-mRNA co-expression (blue); B, upregulated lncRNA-mRNA co-expression (red). Circular, differentially expressed genes; rhombus, differentially expressed long non-coding RNAs.

Figure 3 Competing endogenous RNA network (ceRNA) among differentially expressed long non-coding RNAs, microRNAs and genes. A, downregulated ceRNA axes according to the expression of miRNAs; B, upregulated ceRNA axes according to the expression of miRNAs. Red, upregulated; Blue, downregulated. Circular, differentially expressed genes; rhombus, differentially expressed long non-coding RNAs; triangle, microRNAs.

Figure 4 Protein-protein interaction network. Red, upregulated; Blue, downregulated. Oval, differentially expressed genes; hexagon, differentially expressed transcription factor.

Supplemental Information 1: Raw data.

Supplemental Information 2: All differentially expressed genes.

Supplemental Information 3: LncRNA-mRNA co-expression pairs.

Supplemental Information 4: lncRNA-miRNA-mRNA interaction relationships.

Supplemental Information 5: GO enrichment results of PPI network genes.

Figure 1

Hierarchical clustering and heat map analysis of differentially expressed (A) genes, (B) long non-coding RNAs and microRNAs (C). The color to red, high expression; the color to light blue, low expression.

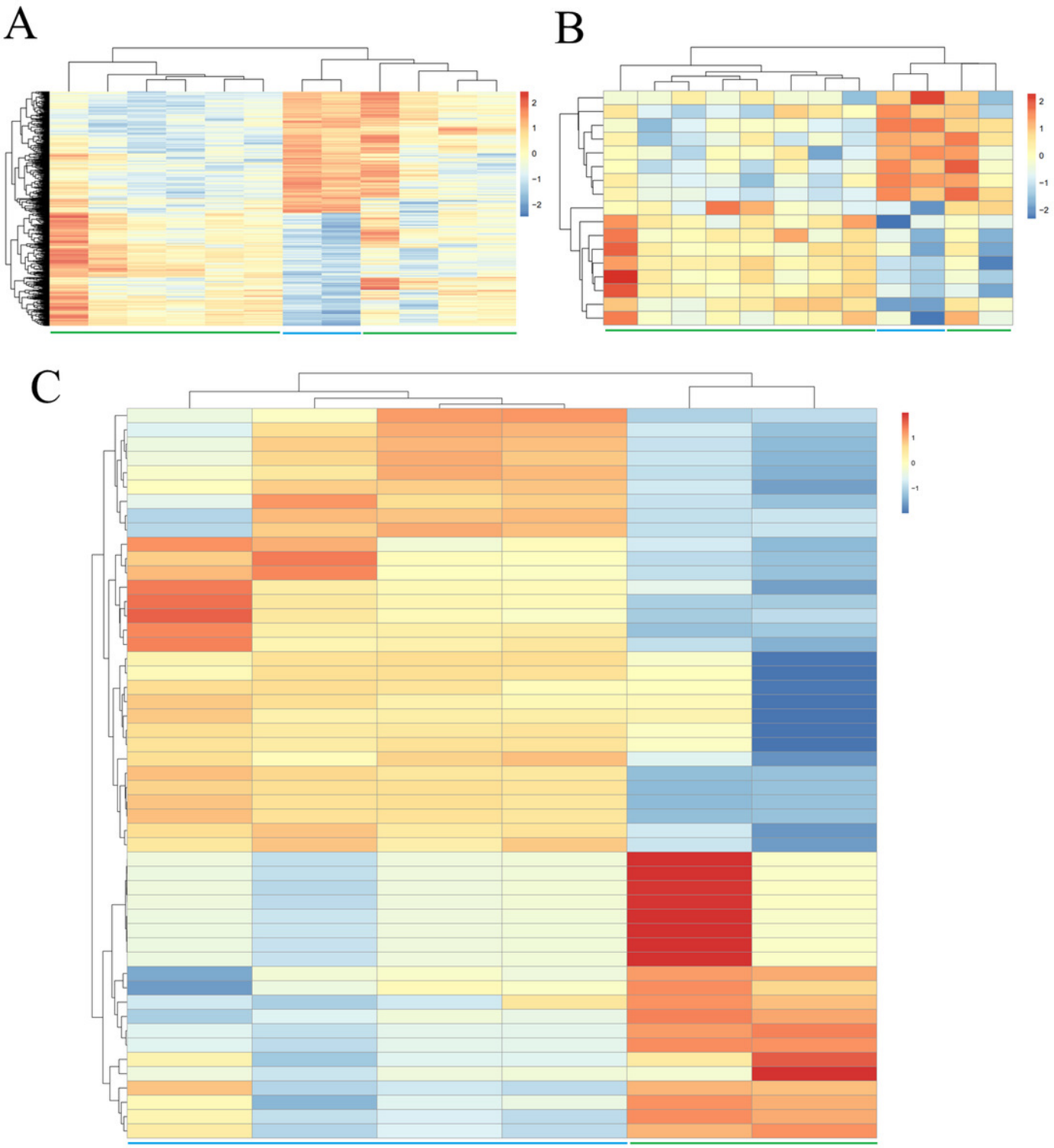
A
B
C

Figure 2

Co-expression network between differentially expressed long non-coding RNAs and genes

A, downregulated lncRNA-mRNA co-expression (blue); B, upregulated lncRNA-mRNA co-expression (red). Circular, differentially expressed genes; rhombus, differentially expressed long non-coding RNAs.

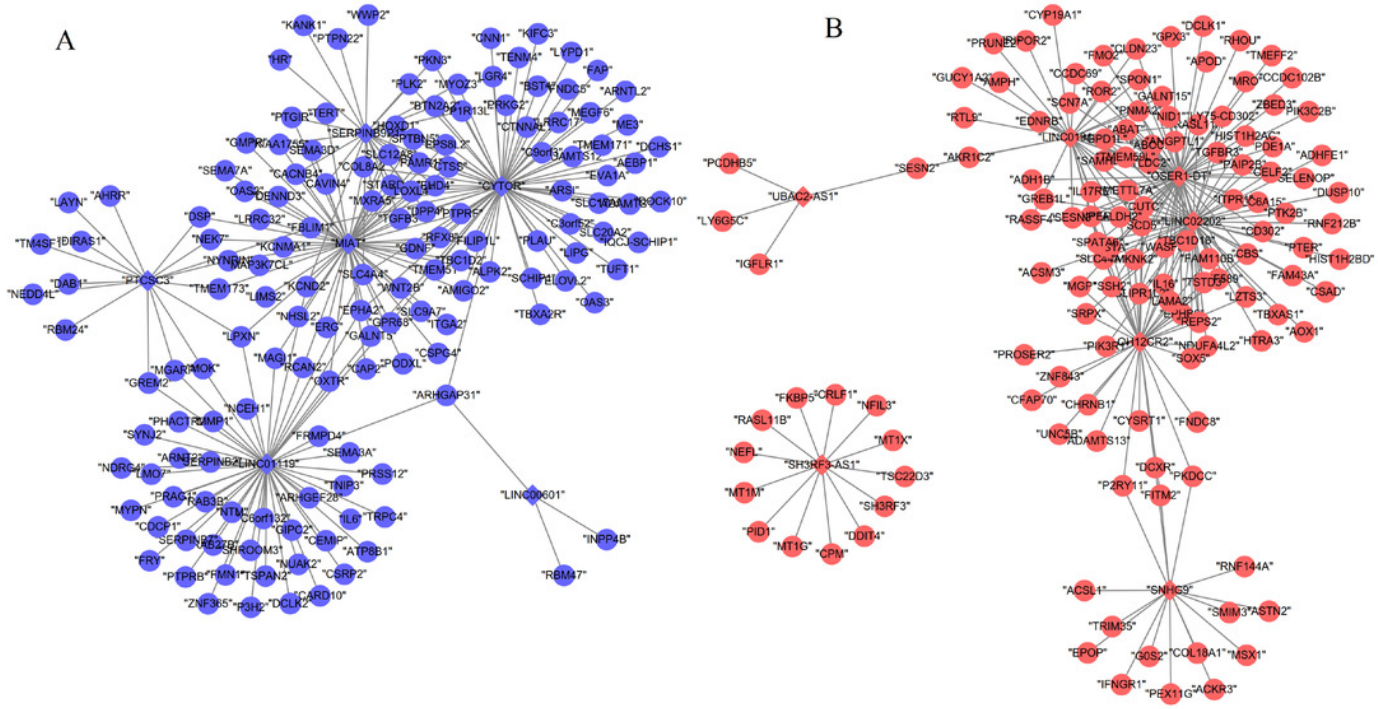

Figure 3

Competing endogenous RNA network (ceRNA) among differentially expressed long non-coding RNAs, microRNAs and genes.

A, downregulated ceRNA axes according to the expression of miRNAs; B, upregulated ceRNA axes according to the expression of miRNAs. Red, upregulated; Blue, downregulated. Circular, differentially expressed genes; rhombus, differentially expressed long non-coding RNAs; triangle, microRNAs.

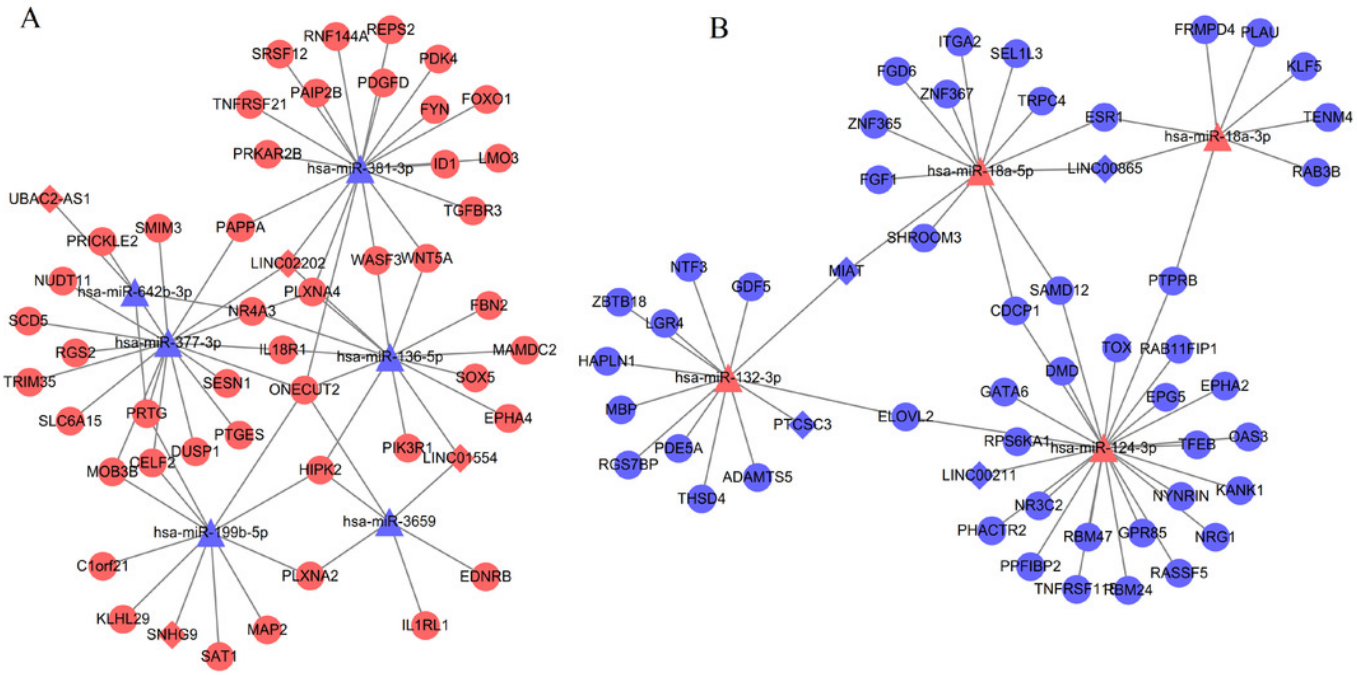

Figure 4

Protein-protein interaction network. Red, upregulated; Blue, downregulated. Oval, differentially expressed genes; hexagon, differentially expressed transcription factor.

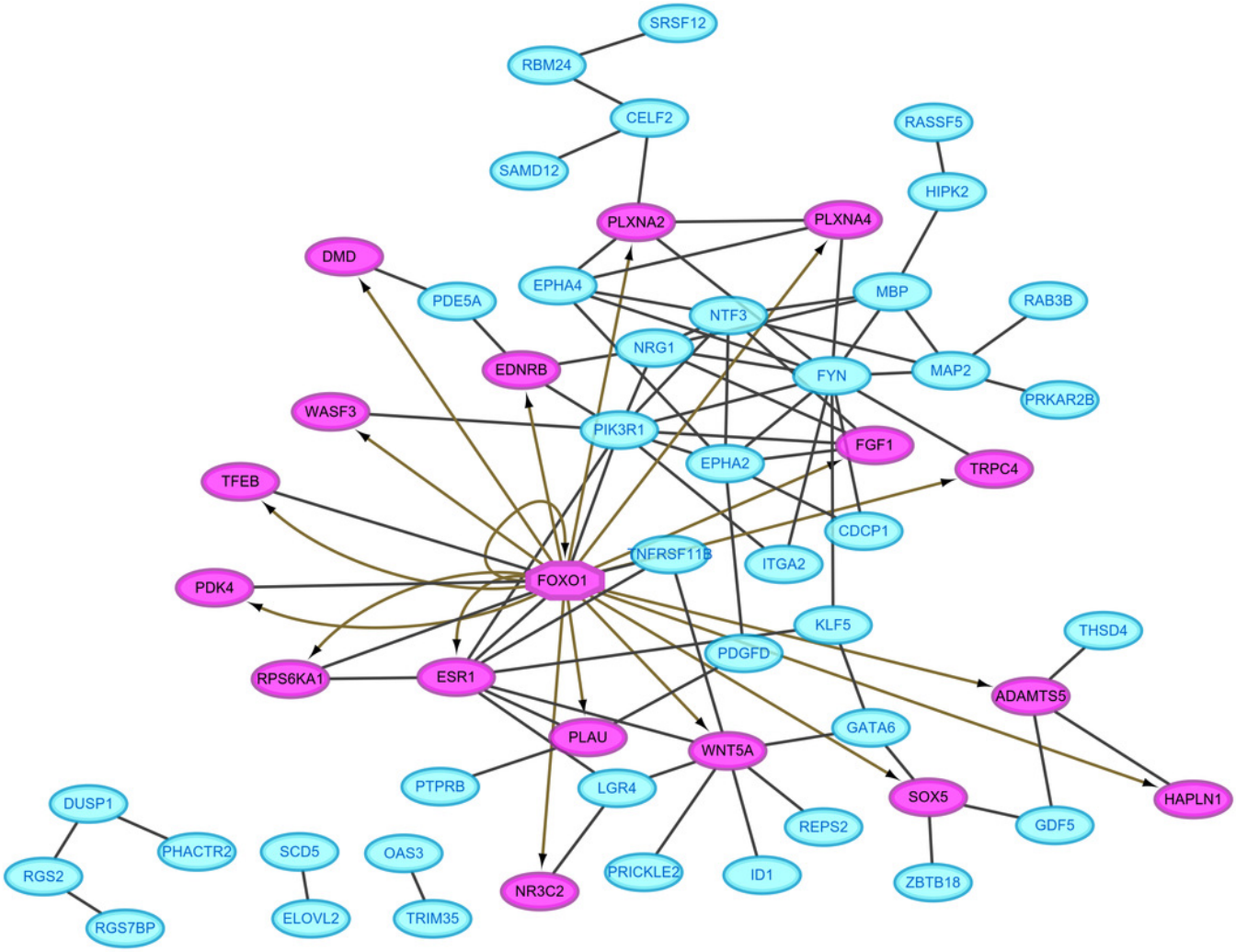

Table 1(on next page)

Differentially expressed genes, lncRNAs and miRNAs

All the differentially expressed miRNAs and lncRNAs were shown, but only top 25 upregulated and downregulated mRNAs as well as crucial genes were displayed. FC, fold change. P-value with asterisk indicated their adjusted p-value were also less than 0.05.

1 **Table 1 Differentially expressed genes, lncRNAs and miRNAs**

	logFC	P-value		logFC	P-value		logFC	P-value
CRLF1	5.31	1.55E-10*	SH3RF3-AS1	4.00	8.45E-06*	miR-663	6.22	2.53E-06*
ZBTB16	6.71	2.90E-10*	LINC01554	2.06	1.19E-02	miR-3607-3p	5.55	3.91E-06*
COMP	6.30	5.07E-10*	SNHG9	2.04	1.45E-02	miR-455-3p	2.93	2.91E-04
FOXO1	4.98	3.85E-09*	LINC01914	2.35	1.74E-02	miR-455-5p	5.68	6.45E-03
LMO3	4.92	5.15E-09*	C18orf65	1.61	2.40E-02	miR-30c	1.45	7.52E-03
KLF15	5.19	6.31E-09*	LINC02202	1.65	4.06E-02	miR-181b	1.45	1.26E-02
MT1G	4.71	1.68E-08*	UBAC2-AS1	1.69	4.17E-02	miR-92a	1.33	1.33E-02
NEFL	5.50	3.12E-08*	LOH12CR2	1.86	4.55E-02	miR-609	2.43	2.97E-02
NRCAM	4.84	5.19E-08*	OSER1-DT	1.92	4.99E-02	miR-339-3p	2.48	2.99E-02
PCSK1	4.32	1.05E-07*	LINC01119	-3.77	1.80E-04*	miR-887	2.65	3.07E-02
FRAS1	6.29	1.14E-07*	SERPINB9P1	-2.35	4.55E-03	miR-124	2.70	3.10E-02
PDK4	5.95	1.50E-07*	MIAT	-3.24	5.06E-03	miR-3653	1.01	3.17E-02
PER1	3.90	3.26E-07*	LINC00601	-1.85	1.98E-02	miR-652	2.90	3.20E-02
IL18R1	4.60	4.67E-07*	LINC00211	-1.48	3.31E-02	miR-769-5p	2.91	3.21E-02
MT1X	3.60	4.76E-07*	PTCSC3	-1.72	3.81E-02	miR-18a	3.08	3.30E-02
MT1M	3.82	4.86E-07*	CYTOR	-1.49	4.63E-02	miR-1290	3.31	3.42E-02
PDE4D	4.06	1.03E-06*	LINC00865	-1.53	4.85E-02	miR-1973	1.15	3.45E-02
SERPINA3	4.91	1.61E-06*	SH3RF3-AS1	4.00	8.45E-06*	miR-30a*	1.84	3.87E-02
RASD1	4.46	1.68E-06*				miR-132	1.23	3.87E-02
IL1RL1	5.91	1.71E-06*				miR-K12-5*	2.93	4.46E-02
GALNT15	4.46	2.24E-06*				miR-150*	-6.28	3.37E-07*
FKBP5	3.42	2.37E-06*				miR-4271	-6.29	1.43E-06*
ELOVL3	3.94	2.95E-06*				miR-371-5p	-6.51	1.79E-06*
HSD11B1	3.63	3.39E-06*				miR-134	-6.39	3.26E-06*
PIK3R1	2.42	5.88E-04				miR-146b-5p	-5.32	4.43E-04
ARNT2	-5.34	3.01E-08*				miR-136	-2.12	1.12E-03
FGF9	-4.24	2.78E-07*				miR-199b-5p	-2.81	4.17E-03
IL6	-5.82	2.90E-07*				miR-29b	-1.80	5.88E-03
OXTR	-5.64	2.06E-06*				miR-376b	-4.36	9.46E-03
RTKN2	-4.16	2.83E-06*				miR-130b	-1.33	1.20E-02
PTPRB	-4.63	4.43E-06*				miR-218	-3.94	1.22E-02
SHROOM3	-3.37	7.27E-06*				miR-154*	-4.42	1.25E-02
RGS4	-3.28	8.10E-06*				miR-381	-1.11	1.31E-02
ARHGEF28	-3.39	1.08E-05*				miR-377	-1.23	1.45E-02
GPR68	-3.67	1.46E-05*				miR-503	-1.85	1.59E-02
VCAM1	-4.30	1.59E-05*				miR-337-5p	-1.04	2.13E-02
ATP8B1	-3.51	1.80E-05*				miR-3132	-1.24	2.18E-02
CNIH3	-3.42	2.61E-05*				miR-362-3p	-3.63	2.18E-02
ZSWIM4	-3.17	2.67E-05*				miR-3659	-1.28	2.23E-02

EPHA2	-3.36	3.35E-05*	miR-H6	-1.49	2.31E-02
CDCP1	-4.48	3.93E-05*	miR-135a*	-2.56	2.37E-02
FRMD5	-3.14	4.35E-05*	miR-29b-1*	-1.79	2.61E-02
NR3C2	-2.88	4.40E-05*	miR-376c	-1.09	2.64E-02
GREM2	-3.48	4.91E-05*	miR-193a-3p	-1.35	2.79E-02
CEMIP	-4.84	4.92E-05*	miR-140-3p	-1.07	2.84E-02
BIRC3	-3.21	8.05E-05*	miR-642b	-3.77	3.04E-02
RBM24	-3.28	9.30E-05*	miR-125a-3p	-1.20	3.16E-02
KY	-3.20	1.08E-04*	miR-140-5p	-1.26	3.51E-02
NUAK2	-2.93	1.21E-04*	miR-718	-2.64	4.41E-02
FGF1	-4.52	1.27E-04*	miR-299-3p	-4.10	4.83E-02
ESR1	-1.911	1.48E-02	miR-376a*	-4.02	4.99E-02

All the differentially expressed miRNAs and lncRNAs were shown, but only top 25 upregulated and downregulated mRNAs as well as crucial genes were displayed. FC, fold change. P-value with asterisk indicated their adjusted p-value were also less than 0.05.

Table 2(on next page)

Hub genes in the protein-protein network screened by topological features

1 **Table 2 Hub genes in the protein-protein network screened by topological features**

Gene	Degree		Betweenness		Closeness		Eigenvector
FYN	12	FYN	983.10	FYN	0.096	FYN	0.42
PIK3R1	10	PIK3R1	716.77	PIK3R1	0.096	PIK3R1	0.39
ESR1	8	ESR1	658.76	KLF5	0.095	NTF3	0.33
NTF3	7	GATA6	543.73	ESR1	0.095	EPHA2	0.32
EPHA2	7	KLF5	529.64	EPHA2	0.093	NRG1	0.30
WNT5A	7	SOX5	438	NRG1	0.093	EPHA4	0.24
NRG1	6	WNT5A	405.05	FOXO1	0.092	FGF1	0.24
FOXO1	6	PLXNA2	352	NTF3	0.092	MBP	0.22
EPHA4	5	CELF2	274	ITGA2	0.092	MAP2	0.18
MBP	5	GDF5	270	GATA6	0.091	ESR1	0.15

2

Table 3(on next page)

KEGG pathway enrichment for the genes in the PPI network.

1 **Table 3 KEGG pathway enrichment for the genes in the PPI network**

Term	P-value	Genes
hsa04015:Rap1 signaling pathway	2.25E-03	RASSF5, ID1, PDGFD, FGF1, PIK3R1, EPHA2
hsa05200:Pathways in cancer	7.28E-03	WNT5A, EDNRB, RASSF5, FOXO1, ITGA2, FGF1, PIK3R1
hsa05205:Proteoglycans in cancer	1.18E-02	WNT5A, ESR1, ITGA2, PIK3R1, PLAU
hsa04014:Ras signaling pathway	1.78E-02	RASSF5, PDGFD, FGF1, PIK3R1, EPHA2
hsa04360:Axon guidance	1.90E-02	EPHA4, FYN, PLXNA2, EPHA2
hsa04390:Hippo signaling pathway	2.97E-02	WNT5A, ID1, GDF5, FGF1
hsa04520:Adherens junction	4.03E-02	PTPRB, WASF3, FYN
hsa05218:Melanoma	4.03E-02	PDGFD, FGF1, PIK3R1

2

Table 4(on next page)

GO biological process term enrichment for the genes in the PPI network

Table 4 GO biological process term enrichment for the genes in the PPI network

Term	P-value	Genes
GO:0042981~regulation of apoptotic process	6.04E-05	RASSF5, TNFRSF11B, DUSP1, NTF3, FYN, GDF5, ESR1
GO:0032148~activation of protein kinase B activity	7.76E-05	WNT5A, NTF3, FGF1, NRG1
GO:0007596~blood coagulation	3.06E-04	PRKAR2B, FYN, GATA6, ITGA2, PDGFD, PLAU
GO:0071560~cellular response to transforming growth factor beta stimulus	5.22E-04	WNT5A, FYN, SOX5, PDGFD
GO:0043066~negative regulation of apoptotic process	6.03E-04	WNT5A, EDNRB, DUSP1, RPS6KA1, ID1, GATA6, FOXO1, PIK3R1
GO:0045944~positive regulation of transcription from RNA polymerase II promoter	1.01E-03	KLF5, WNT5A, RPS6KA1, GATA6, HIPK2, TFEB, ESR1, FOXO1, FGF1, NRG1, PIK3R1
GO:0045893~positive regulation of transcription, DNA-templated	1.25E-03	KLF5, WNT5A, GATA6, HIPK2, TFEB, ESR1, FOXO1, LGR4
GO:0018108~peptidyl-tyrosine phosphorylation	1.47E-03	EPHA4, FYN, FGF1, NRG1, EPHA2
GO:0014066~regulation of phosphatidylinositol 3-kinase signaling	2.02E-03	FYN, FGF1, NRG1, PIK3R1
GO:0030335~positive regulation of cell migration	2.88E-03	NTF3, PDGFD, FGF1, PIK3R1, PLAU
GO:0046854~phosphatidylinositol phosphorylation	3.43E-03	FYN, FGF1, NRG1, PIK3R1
GO:0030182~neuron differentiation	3.53E-03	WNT5A, ID1, HIPK2, EPHA2
GO:0008284~positive regulation of cell proliferation	3.70E-03	KLF5, EDNRB, NTF3, HIPK2, PDGFD, FGF1, NRG1
GO:0048015~phosphatidylinositol-mediated signaling	4.80E-03	FYN, FGF1, NRG1, PIK3R1
GO:0000187~activation of MAPK activity	4.93E-03	WNT5A, NTF3, FGF1, NRG1
GO:0045892~negative regulation of transcription, DNA-templated	5.16E-03	WNT5A, ID1, GATA6, FOXO1, NRG1, ZBTB18,

		LGR4
GO:0045766~positive regulation of angiogenesis	6.02E-03	WNT5A, GATA6, HIPK2, FGF1
GO:0000122~negative regulation of transcription from RNA polymerase II promoter	7.94E-03	KLF5, EDNRB, ID1, GATA6, HIPK2, ESR1, FOXO1, ZBTB18
GO:0043524~negative regulation of neuron apoptotic process	8.79E-03	NTF3, FYN, GDF5, HIPK2
GO:0035556~intracellular signal transduction	9.37E-03	PRKAR2B, RASSF5, DUSP1, RPS6KA1, FYN, NRG1
GO:0045213~neurotransmitter receptor metabolic process	9.62E-03	DMD, NRG1
GO:0060750~epithelial cell proliferation involved in mammary gland duct elongation	1.28E-02	WNT5A, ESR1
GO:0048146~positive regulation of fibroblast proliferation	1.31E-02	WNT5A, ESR1, PDGFD
GO:0043406~positive regulation of MAP kinase activity	1.54E-02	PDE5A, PDGFD, FGF1
GO:0043627~response to estrogen	1.86E-02	TNFRSF11B, GATA6, ESR1
GO:0014068~positive regulation of phosphatidylinositol 3-kinase signaling	1.86E-02	FYN, PDGFD, NRG1
GO:0048841~regulation of axon extension involved in axon guidance	2.23E-02	PLXNA4, PLXNA2
GO:0008366~axon ensheathment	2.23E-02	NRG1, MBP
GO:0050966~detection of mechanical stimulus involved in sensory perception of pain	2.54E-02	FYN, ITGA2
GO:0008286~insulin receptor signaling pathway	2.61E-02	PDK4, FOXO1, PIK3R1
GO:0090630~activation of GTPase activity	2.67E-02	WNT5A, NTF3, EPHA2
GO:0060068~vagina development	2.89E-02	WNT5A, ESR1
GO:0021785~branchiomotor neuron axon guidance	2.86E-02	PLXNA4, PLXNA2
GO:0007165~signal transduction	3.11E-02	TNFRSF11B, NTF3, RPS6KA1, PDE5A, NR3C2, ESR1, FGF1, PIK3R1, PLAU

GO:0048013~ephrin receptor signaling pathway	3.12E-02	EPHA4, FYN, EPHA2
GO:0031643~positive regulation of myelination	3.17E-02	WASF3, NRG1
GO:0010976~positive regulation of neuron projection development	3.33E-02	WNT5A, FYN, DMD
GO:1901653~cellular response to peptide	3.48E-02	KLF5, ID1
GO:0046849~bone remodeling	3.48E-02	LGR4, EPHA2
GO:0033628~regulation of cell adhesion mediated by integrin	3.48E-02	EPHA2, PLAU
GO:0001525~angiogenesis	3.49E-02	KLF5, PTPRB, ID1, FGF1
GO:0007179~transforming growth factor beta receptor signaling pathway	3.53E-02	ID1, GDF5, HIPK2
GO:0008584~male gonad development	3.68E-02	WNT5A, GATA6, ESR1
GO:1902287~semaphorin-plexin signaling pathway involved in axon guidance	3.79E-02	PLXNA4, PLXNA2
GO:0055119~relaxation of cardiac muscle	3.79E-02	RGS2, PDE5A
GO:0007169~transmembrane receptor protein tyrosine kinase signaling pathway	3.82E-02	NTF3, FYN, NRG1
GO:0001678~cellular glucose homeostasis	4.41E-02	FOXO1, PIK3R1
GO:0060065~uterus development	4.41E-02	WNT5A, ESR1
GO:0006636~unsaturated fatty acid biosynthetic process	4.72E-02	ELOVL2, SCD5

2